Available online at www.sciencedirect.com
SCIENCE DIRECT®
Journal of the European Ceramic Society 25 (2005) 559–567
www.elsevier.com/locate/jeurceramsoc

Effect of sintering additives on the oxidation behavior of Si_3N_4 ceramics at 1300 °C

K. Houjou [a], K. Ando [b,*], M. C. Chu [b], S. P. Liu [c], S. Sato [d]

[a] *Yokohama National University, 79-5 Hodogaya, Yokohama, Japan*
[b] *Department of Energy and safety Engineering, Yokohama National University, 79-5 Hodogaya, Yokohama, Japan*
[c] *Department of Mechanical Engineering, Ching-Yun University, 229 Chien-Hsin Rd., 32049 Jung-Li, Taiwan, R.O.C.*
[d] *NHK Spring Co. Ltd., 3-10 Fukuura Kanazawaku, Yokohama, Japan*

Received 19 September 2003; received in revised form 11 March 2004; accepted 21 March 2004
Available online 11 June 2004

Abstract

This paper describes the results of systematic investigation of the oxidation behavior of Si_3N_4 based ceramics. The tests were carried out at 1300 °C for 2000 h in a high-temperature dry air environment. The Si_3N_4 specimens tested include the following: (a) S-1: Si_3N_4 added 8 mass% Y_2O_3, (b) S-2: Si_3N_4/SiC added 8 mass% Y_2O_3, (c) S-3: Si_3N_4 added 5 mass% Y_2O_3 and 3 mass% Al_2O_3, (d) S-4: Si_3N_4/SiC added 5 mass% Y_2O_3 and 3 mass% Al_2O_3. Several interesting conclusions were obtained as follows: (1) the thicknesses of oxidized layer of S-3 and S-4 were much thicker than S-1 and S-2, (2) oxidation kinetics of S-1 and S-2 obeyed a parabolic law on the whole, while those of S-3 and S-4 had a break, (3) the yttrium (Y) concentration under the oxidized layer decreased significantly. The Y-decreased zone was defined as a diffused layer. The thicknesses of the diffused layers of S-3 and S-4 samples were very large. (4) Primarily, the crystalline phases in the oxidized layer were SiO_2 and $Y_2Si_2O_7$. (5) The effect of SiC composition on the oxidation behavior was small.

Keywords: Si_3N_4; Additive powder; Oxidation; Diffusion; Y_2O_3; Al_2O_3

1. Introduction

In recent years, silicon nitride ceramics have been used in the structural members of gas turbine, engines and other parts subjected to high-temperature conditions. However, non-oxide ceramics, which are based on silicon nitride, are weak in high-temperature oxidizing environments, and their strength progressively weakens in such oxidizing conditions. Much research concerning the behavior of oxidation at high-temperature has been done. This research shows the importance of mechanical properties such as fatigue strength and high-temperature strength. These properties are considered important guidelines for the design plan of structural ceramic members at high temperature. However, most oxidation studies were conducted for less than 1000 h. This short experiment time is not enough for structural members.

It is well-known that additives and sintering powders have a major effect on the oxidation behavior and high-temperature strength of structural ceramics.[1–6]

In this study we are preparing four kinds of Si_3N_4-based ceramics, including Y_2O_3 and Al_2O_3 (both for sintering powders) and SiC. The oxidation was carried out at 1300 °C for 2000 h in the atmosphere. The kinetics of thickness of oxidized layer, oxide and its changing appearance, the change of base ceramic material and other factors were investigated.

2. Material, specimens and experimental method

2.1. Material and specimens

The starting powder used in this investigation has the following properties:

(a) The mean particle size of Si_3N_4 powder (EBE SN-E-10) is 0.2 μm and its specifications are shown in Table 1.
(b) The β-SiC powder used as composition has a 0.27 μm mean particle size.
(c) Y_2O_3 and Al_2O_3 are used as sintering additive powders.

Thus, including SiC, four types of preliminary powder were prepared.

* Corresponding author. Fax: +81-45-339-4024.
E-mail address: andokoto@ynu.ac.jp (K. Ando).

0955-2219/$ – see front matter © 2004 Elsevier Ltd. All rights reserved.
doi:10.1016/j.jeurceramsoc.2004.03.023

Table 1
Specifications of Si_3N_4 powder (Ube SN-E-10)

Impurities	
O (wt.%)	1.31
Cl (ppm)	<100
Fe (ppm)	<100
Ca (ppm)	<50
Al (ppm)	<50
$\beta/(\alpha+\beta)$ (wt.%)	<5
Crystallinity (wt.%)	>99.5

These nomenclature of specimens and their properties are described as follows:

(1) S-1: Additive powder is 8 mass% Y_2O_3.
(2) S-2: Composite powder is 20 mass% SiC, additive powder is 8 mass% Y_2O_3.
(3) S-3: Additive powders are 5 mass% Y_2O_3 and 3 mass% Al_2O_3.
(4) S-4: Composite powder is 20 mass% SiC, additive powders are 5 mass% Y_2O_3 and 3 mass% Al_2O_3.

To this mixture, alcohol was added and blended thoroughly for 48 h. The mixture was placed into an evaporator to extract the solvent, and then put into a vacuum to produce a dry powder mixture. The mixture was subsequently hot-pressed at 1850 °C and 35 MPa for 1 h in nitrogen gas. The surface of the sintered specimen was mirror finished by lapping after grinding, and the surface roughness Ry (JIS)[7] of the specimen was 0.05 μm.

2.2. Experimental method

The oxidation was carried out under atmosphere environment (completely dry air) in an electric furnace. All oxidation was at 1300 °C. The oxidation time was divided into four groups: 100, 500, 1000, and 2000 h. The samples were heated with increase-rate of 10 °C/min up to 1300 °C, and then cooled down in an electric furnace after keeping this temperature for 100 h. The oxidation time (t_o) was defined by the accumulated times of this cycle: 1 time, 5 times, 10 times, and 20 times.

The surface of the oxidized specimens was observed by SEM. The oxidation products were identified and investigated by X-ray diffraction (XRD) and electron probe micro analyzer (EPMA). Where, the conditions of XRD measurement were as follows: (1) characteristic X-ray; Cu-$K_{\alpha1}$, (2) tube current; 60 mA, (3) tube voltage; 50 kV.

Next, specimens were sliced perpendicularly to the oxidized layer, then put into resin and hardened in vacuum. Surface of the slice was mirror finished by diamond paste lapping (grain diameter: rough = 9 μm, finished = 1 μm). The concentrations of yttrium (Y), aluminum (Al), silicon (Si), and oxygen (O), were mapped by EPMA. Then SEM was used to observe the microstructure. These methods were the basis for our evaluation of the reacted (i.e., oxidized) layer.

3. Test results and discussion

3.1. SEM observations of oxidized surfaces

Fig. 1 shows the SEM photographs of oxidized surfaces of S-2 that was sintered with Y_2O_3 as an additive powder and SiC as a composite powder. Fig.1(a) shows the initial condition. Fig. 1(b) shows the $t_o = 100$ h condition, very small particles just appear on the surface. But in Fig. 1(c) $t_o = 500$ h, the specimen's surface is completely covered with glassy oxide, and crystalline materials are observed. The mean grain diameter is about 4 μm. As a result of EPMA and XRD measurement, this newly formed material was recognized as SiO_2 (α-cristobalite), and this discovery will be mentioned later in detail. A slight amount of $Y_2Si_2O_7$ (yttrium silicate) is also detected. In Fig. 1(c) $t_o = 500$ h and Fig. 1 (d) $t_o = 2000$ h, many cracks in a testudinate pattern are observed on the oxidized surface. These were caused by the difference of the coefficient thermal expansion between base material and oxidized layer during cooling down procedure. Also, when observing the cross section, cracks exist only at the oxidized layer, and cracks do not penetrate into the base material. The morphology of produced oxide of S-1 seemed to be almost the same as S-2.

Fig. 2 shows the SEM photographs of the oxidized surfaces of S-3 obtained by sintering with Y_2O_3 and Al_2O_3 as additive powders. Fig. 2(a) is the initial condition. Looking at Fig. 2(b), when $t_o = 100$ h, the specimen's surface is completely covered with oxide. This oxidized surface is glass phase with small crystals. As mentioned later, this crystalline phase was recognized as $Y_2Si_2O_7$, but the phase around this crystal phase was glass consisting of Si, O, Al, etc. Moreover, several holes are scattered on the oxide surface. In the case of S-4, a few similar holes can be observed. These holes seem to be created by gas egress through the oxidized layer, and this gas was generated by the reaction between Si_3N_4, SiC, and O_2. As mentioned above, SiO_2 and $Y_2Si_2O_7$ seem to be generated from Eqs. (1) to (5).

$$Si_3N_4 + 3O_2 \rightarrow 3SiO_2 + 2N_2\,(g) \quad (1)$$

$$SiC + \tfrac{3}{2}O_2 \rightarrow SiO_2 + CO(CO_2)\,(g) \quad (2)$$

$$\tfrac{2}{3}Si_3N_4 + Y_2O_3 + 2O_2 \rightarrow Y_2Si_2O_7 + \tfrac{4}{3}N_2\,(g) \quad (3)$$

$$2SiC + Y_2O_3 + 3O_2 \rightarrow Y_2Si_2O_7 + CO(CO_2)\,(g) \quad (4)$$

$$Y_2O_3 + 2SiO_2 \rightarrow Y_2Si_2O_7 \quad (5)$$

In Fig. 2(c) and (d), the stick-shape crystal of $Y_2Si_2O_7$ has remarkably grown larger, and its length almost reaches 100 μm. The gas holes, as mentioned before, have almost disappeared from the surface. Sample S-4 shows oxidation behavior that is the same as for sample S-3.

As discussed above, most oxidized layers, obtained from four kinds of silicon nitride, had a dual structure including a crystalline phase and a glassy phase. It was recognized that

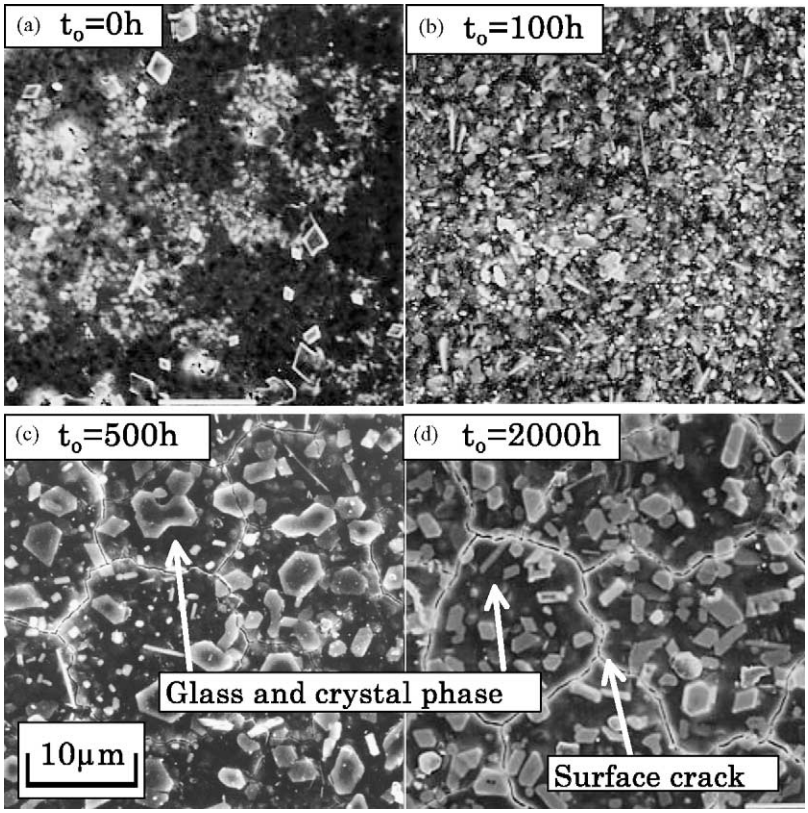

Fig. 1. SEM photographs of oxidized layer surface of S-2.

the $Y_2Si_2O_7$ crystals become larger, especially in S-3 and S-4 samples using Y_2O_3 and Al_2O_3 as sintering additives. However, it is believed that adding SiC has very few effects on the oxidation behavior.

3.2. X-ray diffraction (XRD) results of oxidized surfaces

In order to investigate the oxide and its degree of crystallinity, XRD measurement was carried out. All of the measurement area was unified to size 4 mm × 8 mm. XRD profiles were dependent on the kind of additive powders used, in the same way as SEM observation in Section 3.1. The XRD results of specimen's surface are shown in Fig. 3. The sample S-1 at t_o = 500 h is shown in Fig. 3(a). The peak ($2\theta = 22^\circ$ (●)) of SiO_2: α- cristobalite (1 0 1) is diffracted most intensely expect the peaks of the base material. Also, a slight amount of $Y_2Si_2O_7$ is detected. Meanwhile, sample S-2 with added SiC showed similar behavior to sample S-1. On the other hand, Fig. 3(b) shows the S-4 sample at t_o = 100 h. In the S-4 case, the peak ($2\theta = 16.5^\circ$ (▲)) of $Y_2Si_2O_7$ (1 1 0) is diffracted intensely, and also a slight amount of SiO_2 is detected. However, when considering the relationship between Fig. 2(c) and (d) and the XRD results, the identification of the phase surrounding the $Y_2Si_2O_7$ crystal is almost a glass phase. As for the S-3 sample, the XRD result was approximately the same as the above-mentioned S-4 sample.

The peaks of SiO_2 (1 0 1) and $Y_2Si_2O_7$ (1 1 0) in Fig. 3 help to form an understanding of the relationship between oxidation time and intensity of XRD on the surface of oxidized specimens. It seems that there is higher reliability, because these peaks are not affected by the Si_3N_4 peaks. The relationships between oxidation time (t_o) and the intensity (cps) of XRD peaks are shown in Fig. 4. Fig. 4(a) shows the SiO_2 (1 0 1) peaks. The intensities of S-1 (●) and S-2 (▲) using Y_2O_3 as an additive increase with increasing oxidation time. On the contrary, the peaks of S-3 (○) and S-4 (△) using Y_2O_3 and Al_2O_3 as additives are detected until t_o = 100 h, but these peaks disappear after that time. In general, impurities concentrate on the oxidized layer during oxidation.[1,8,11] In this experiment, using the EPMA analysis on the oxidized layer, particularly for S-3 and S-4, other low-melting point impurities, i.e., K, Ca, Na, Mg, beside Y and Al, were detected. Taking into consideration these facts, it seems that it is hard to crystallize SiO_2. Fig. 4(b) shows the $Y_2Si_2O_7$ (1 1 0) peaks. The peaks of S-3 (○) and S-4 (△) increase with increasing oxidation time. While the peaks of S-1 (●) and S-2 (▲) are hardly detected from beginning to end.

Considering the above-mentioned circumstances, the following two results could help to explain the crystal production in the oxidized layer. (1) With regard to S-1 and S-2 using only Y_2O_3 as an additive, the SiO_2 was produced in proportion to oxidation time, while the

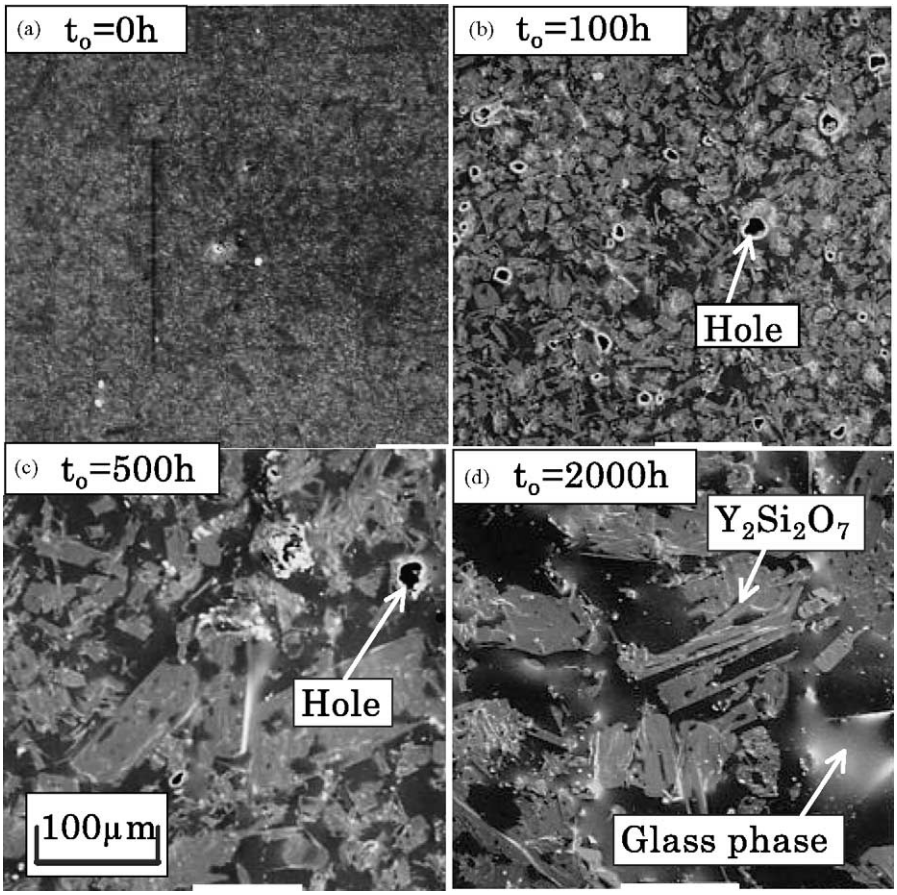

Fig. 2. SEM photographs of oxidized layer surface of S-3.

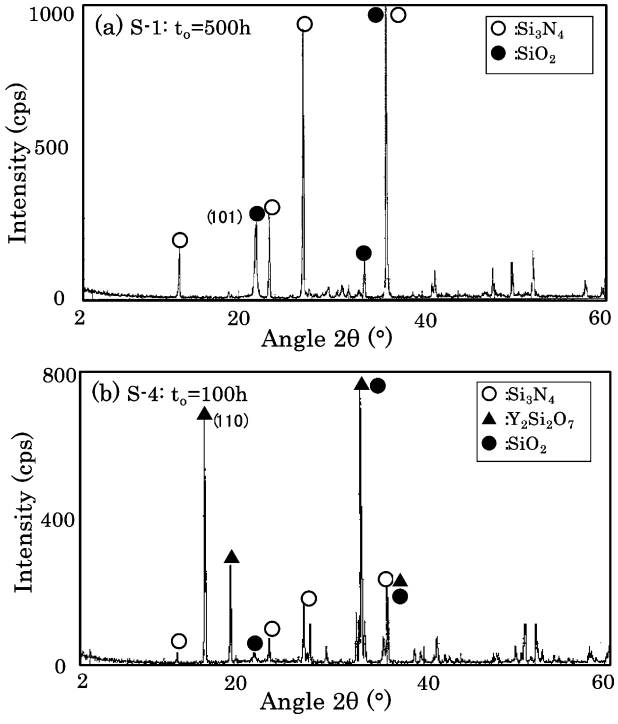

Fig. 3. Results of XRD: (a) S-1, $t_o = 500$ h and (b) S-4, $t_o = 100$ h.

$Y_2Si_2O_7$ was meagerly produced. However, the effects of SiC composition on these behaviors were not clear. (2) Regarding S-3 and S-4 using Y_2O_3 and Al_2O_3 as additives, the $Y_2Si_2O_7$ was produced in proportion to oxidation time, but the amount of produced SiO_2 was very small.

3.3. SEM and EPMA observation on the sample cross section

Next, specimens were perpendicularly cut through the oxidized surface, and then they were mirror polished and observed by SEM and EPMA. Fig. 5 shows the SEM photographs of cross sections of the oxidized layer which are obtained from each specimens at $t_o = 1000$ h. In Fig. 5(a) S-1 and Fig. 5(b) S-2, many cracks are found at the oxidized layer. These cracks did not occur during oxidation but during the lapping process. These cracks make it difficult to measure the thickness of oxidized layer in some specimens. For these reasons the thickness of oxide was measured by SEM photographs and EPMA oxygen mapping. Fig. 6 shows the SEM photograph and EPMA oxygen mapping which correspond to each other. From these results, it is obvious that the SEM observed the thickness of ox-

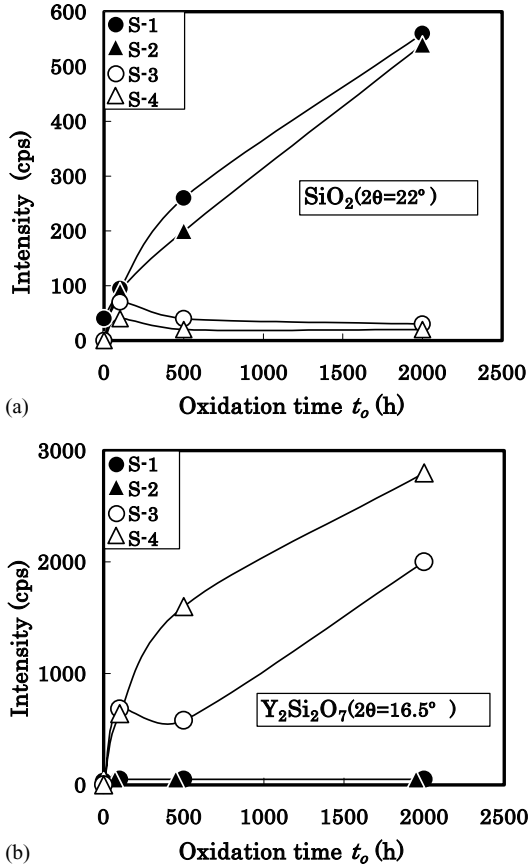

Fig. 4. Relationship between oxidation time (t_o) and intensity of XRD on surface of oxidized specimens: (a) SiO_2; $2\theta = 22^\circ$ and (b) $Y_2Si_2O_7$; $2\theta = 16.5^\circ$.

ide and EPMA measured rich oxygen layer are in agreement.

In Fig. 5(a) and (b), the oxidized layers of S-1 and S-2 show very little growth, despite $t_o = 1000$ h oxidation. On the other hand, the thickness of the oxidized layers of S-3 and S-4 have grown to several tens of micrometers, producing large crystals ($Y_2Si_2O_7$) inside the layer. When comparing S-3 with S-4, which both used the same additives (Y_2O_3 and Al_2O_3), the thickness of oxidized layer of S-3 without SiC added is larger than that of S-4. However, when comparing S-1 with S-2 using Y_2O_3 as an additive, very little difference is found. In addition, many pores are observed in the range of 20–40 μm from the oxide/ceramics interface of S-3. In Fig. 5(d) S-4, a large number of pores are found, but the observation is not clear because of its contrast. Many pores exist near where $Y_2Si_2O_7$ grows in very thick oxide. Yet size and frequency of generated pores are so uneven, that the quantitative relationship between oxidation time and thickness is difficult. However, in Fig. 5(a) and (b), these pores were not observed.

In conclusion, in the case of samples using Y_2O_3 and Al_2O_3 as additives, the oxidized layer grew very thick and the effect on the base material was revealed. But in the case of samples that used only Y_2O_3 as an additive, the oxidized or reacted layer was very small. Consequently, it is concluded that the oxidation resistance of S-2 is excellent.

3.4. Oxidation behavior

In many case studies, discussions of oxidation behavior are based on weight-change measurement of specimens.[1–5,8,9] In this study, the oxide thickness was measured directly, and the general behaviors were investigated too. As is obvious from Eqs. (1) to (4) in Section 3.1, the oxidation reactions are complicated. The oxidation of Si_3N_4 ceramics incorporates with oxygen; it generates and releases several kinds of gas. Therefore, the weight of specimen does not simply increase, and secondary reaction by-products are expected. Considering the above-mentioned, it is appropriate to study the oxidation property that the assessment depends on the volume (=thickness) of oxide, comprehensively.

In this study, as mentioned in Fig. 6 (Section 3.3), the thickness of oxidized layers were measured by SEM photographs and EPMA oxygen mapping, as shown in the cross section of oxidized layer. Fig. 7(a) shows the relationship between oxidation time (t_o) and thickness of the oxidized layer (T_o). According to this figure, the increase-rate of the oxide thickness of S-3 (○) is the fastest, and S-2 (▲) is the slowest. It is discovered that sintering additives have a large effect on the thickness of oxidized layer. The oxide thickness of S-1 (●) and S-2 (▲) added Y_2O_3 increase slightly. Specifically, the increase is only 1 or 2 μm per 1000 h for the later experiment. Also, finally for $t_o = 2000$ h, the thickness is only several micrometers. However, oxidized layers of S-3 (○) and S-4 (△) added both Y_2O_3 and Al_2O_3 grow very thick. Finally for $t_o = 2000$ h, they have several tens of micrometers.

In addition, the rate of increase in the thickness of oxidized layer of the sample with added SiC was smaller than other sample. It is concluded that the effect of SiC addition is less than the effect of Al_2O_3 addition.

In the oxidation reaction as mentioned above, it is necessary that the penetrant move through oxidized layer. Therefore, the rate of increasing oxide thickness $d(T_o)/d(t_o)$ is in inverse proportion to the oxide thickness. Thus, dependence on time to thickness follows a parabolic reaction rate law:

$$T_o^2 = kt_o \quad (6)$$

where k is reaction constant. Fig. 7(b) shows the relationship between square root of time $(t_o)^{1/2}$ and oxide thickness (T_o). According to this relation, S-1 and S-2 generally obey a parabolic characteristic. On the other hand, S-3 and S-4 have a break between $t_o = 500$ and 1000 h, in spite of small number measuring points. When the oxidation has been continued long time, its kinetics does not always obey only one parabolic rate, which many studies explain.[6,9–11]

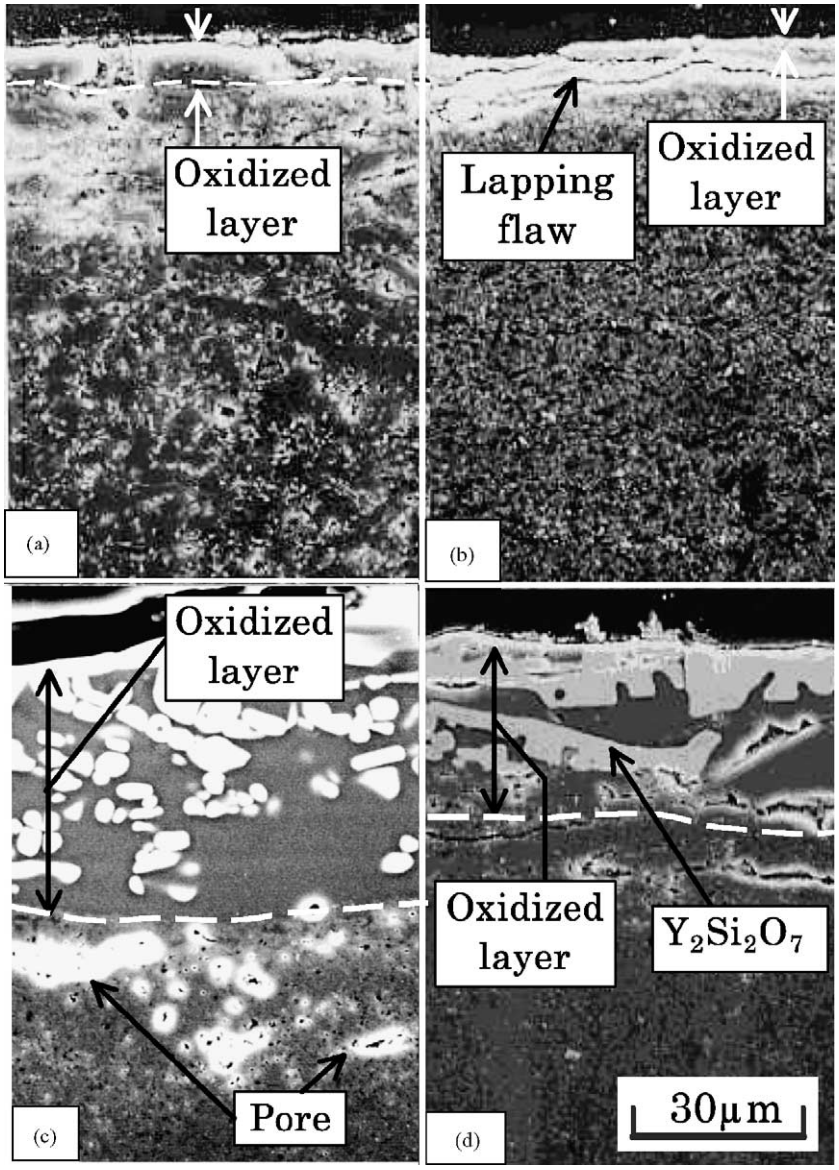

Fig. 5. SEM photographs of oxidized layer $t_o = 1000$ h: (a) S-1, (b) S-2, (c) S-3, and (d) S-4.

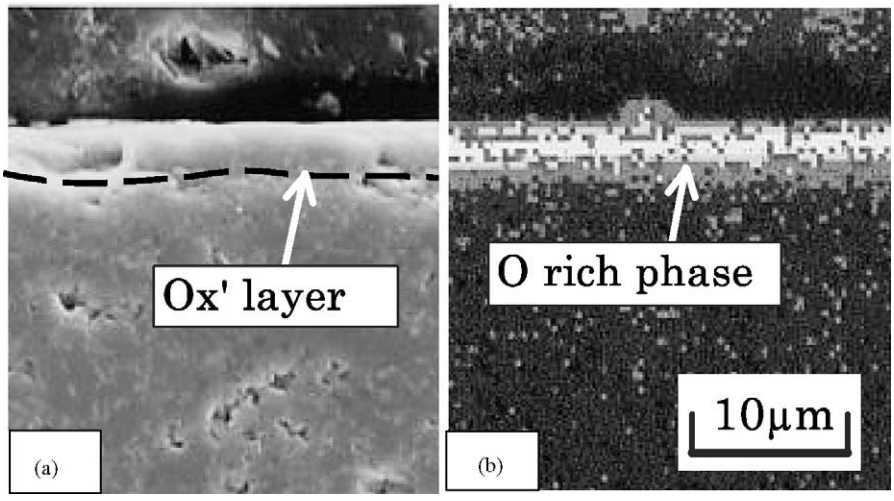

Fig. 6. Photographs of oxidized layer S-1, $t_o = 500$ h: (a) SEM and (b) EPMA mapping of O.

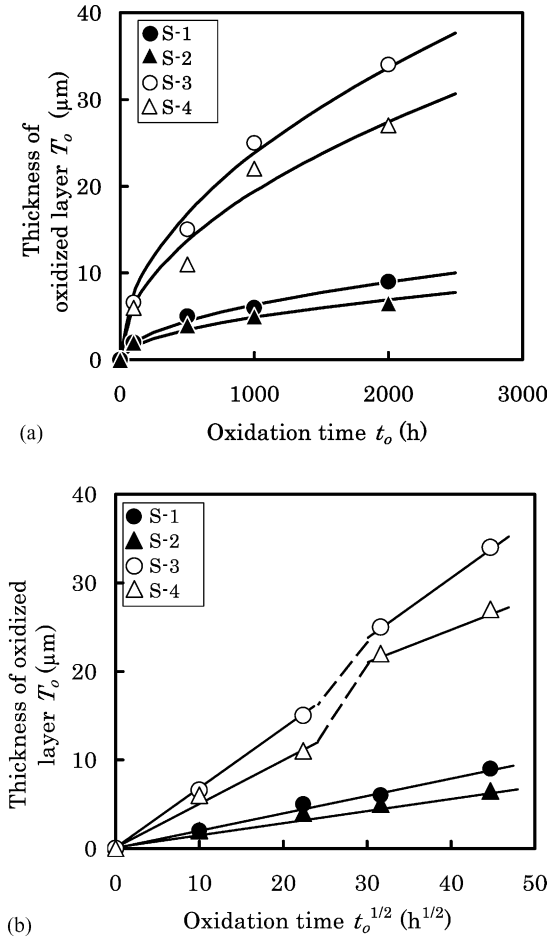

Fig. 7. Oxidation kinetics. (a) Relationship between oxidation time (t_o) and thickness of oxidized layer (T_o). (b) Relationship between the square root of time $(t_o)^{1/2}$ and thickness of oxidized layer (T_o).

Therefore, the breaks appear frequently in experiments. In present study, certain reasons being not clear, the breaks are seem to be caused by difference of the oxidation mechanism between before and after the break. Main difference is following. Note Fig. 2(b) and (c), many pores exist on the oxide until $t_o = 500$ h, and they supply air for oxidation. However, above $t_o = 500$ h, these pores disappear, the breaks appear in the same time.

In addition, the oxide volume grows immediately near this changing point. The volume growth seems to be caused by embedding of the generated gas such as N_2 in the oxide, which Oliveira[9] et al. describe. Therefore bubbles exist inside the oxide. According to the observation of cross sections, the oxides of S-3, S-4 are dense until $t_o = 500$ h, while they look like comparatively porous after $t_o = 1000$ h.

3.5. Thickness of the diffused layer inside base material

The concentration distributions of O, Al, Si, and Y at the oxidized layer of the cross section are measured by EPMA. Fig. 8 shows the distribution of Y by maps of all specimen types after 2000 h of oxidation treatment. The concentration of Y is so high that it appears white (to the right) in this figure. In Fig. 8(a) and (b), any variations in the concentration of Y cannot be discerned within the base material. By contrast, in Fig. 8(c) and (d) dark (black) area with a 20–30 μm thickness shows a discernible distribution pattern. The concentration of Y is low and is observable at a considerable depth under the oxidized layer. This area indicates a diffused layer (T_d) having a distinct oxidized layer. Another observation is that the distribution of Al has a similar appearance, although on a smaller scale. Despite these features, a distinct interface like the Y-diffused layer dose not exist. It is impossible to quantify an area of low concentration in terms of the thickness of a diffused layer. Comparing Fig. 5 with 8 it is inferred that Y, Al and other elements have migrated significantly from the grain boundaries in the diffused layers to the oxidized layers. Therefore, it is concluded that the concentrations of these elements decreased near the oxidized layer. This tendency is evident particularly for S-3 (○) and S-4 (△) both with added Y_2O_3 and Al_2O_3. Babini et al. explain that Si_3N_4/Y_2O_3 ceramics have good oxidation resistance because of the refractoriness (high viscosity) of the grain boundary phase.[2] And this explanation help to understand the results of EPMA mappings in Fig. 8. Also, this region is closely coincident with the regions of high pore generation as shown in Fig. 5(c). Consequently it is inferred that these pores were produced in areas where large amounts of Y and Al were diffused and distributed. The thickness of the S-4 diffused layer with added SiC is about 20–40% smaller than the thickness of S-3 without added SiC.

Fig. 9 shows the relationship between oxidation time (t_o) and thickness of Y-diffused layers (T_d), obtained from the measured results. With S-1 and S-2, as mentioned before, the diffused layer does not exist. On the other hand, for S-3 (○) and S-4 (△), the thickness of diffused layer (T_d) increase with increasing oxidation time (t_o). In addition, the thickness of diffused layer of S-4 (△) added SiC is about 25% smaller than the thickness of S-3 (○). However, the effect of SiC is less than that of the sintering additive, like the case of the oxidized layer.

Fig. 10 shows the relationship between the thickness of the oxidized layer (T_o) and the thickness of Y-diffused layer (T_d). S-3 (○) and S-4 (△) are in proportional in the whole, as represented in Eq. (7).

$$T_d = 0.85T_o \tag{7}$$

From the above-mentioned circumstances, the rate of increasing the thickness of oxidized layer on S-1and S-2 was controlled by diffusion inside the oxidized layer. On the other hand, the rate of increasing on S-3 and S-4 was controlled by the diffusion of metallic ions, i.e., Y, Al and others which move through the grain boundary of the base material, in addition to the diffusion in the oxidized layer.

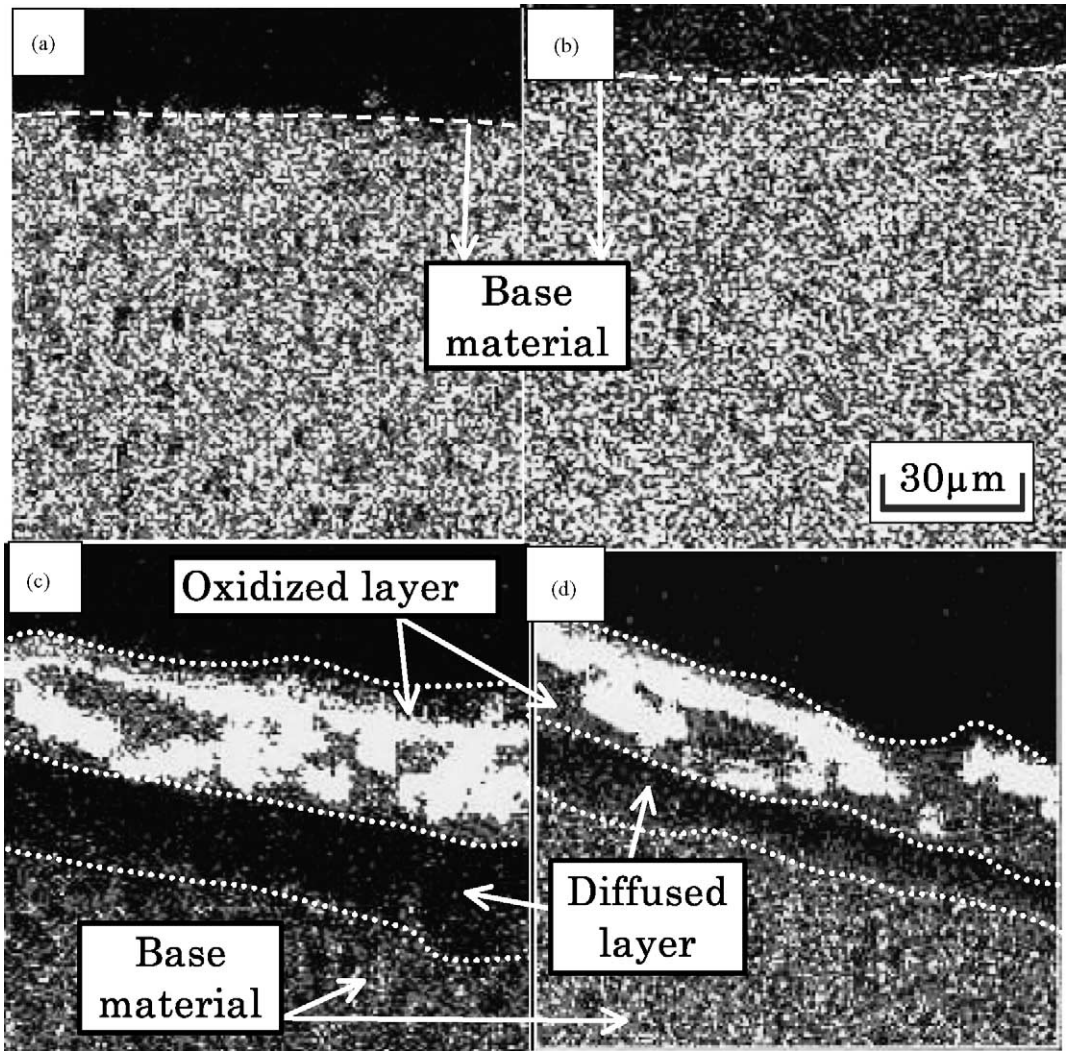

Fig. 8. EPMA mappings of Y, $t_o = 2000$ h: (a) S-1, (b) S-2, (c) S-3, and (d) S-4.

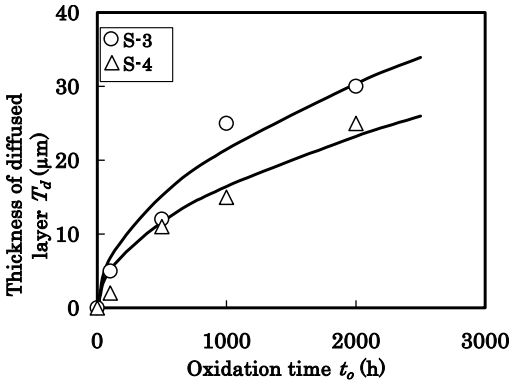

Fig. 9. Relationship between oxidation time (t_o) and thickness of Y diffused layer (T_d).

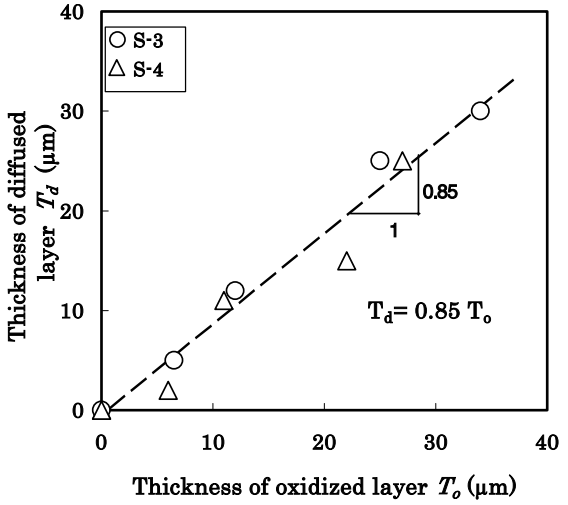

Fig. 10. Relationship between thickness of oxidized layer (T_o) and Y diffused layer (T_d).

4. Conclusions

Using four kinds of Si_3N_4-based ceramics, oxidation experiments were carried out at 1300 °C for 2000 h in an atmosphere environment. The effects of an addition (SiC) and sintering additives on oxidation behavior were investigated. The main conclusions are as follows:

(1) SEM surface examination of many specimens showed that the oxidized layer consists of a dual structure made of a glassy phase and a crystalline phase.
(2) Analysis of oxide by XRD showed that if the specimen had Y_2O_3 as a sintering additive, then the crystalline phase was SiO_2 (α-cristobalite), and the quantity increased with increasing oxidation time. However, if the specimen had both Y_2O_3 and Al_2O_3 as sintering additives, then the crystalline phase was yttrium-silicate ($Y_2Si_2O_7$), and the quantity increased with increasing oxidation time.
(3) The thicknesses of oxidized layers differed greatly depending on the difference of sintering additives. In the case of samples that had only Y_2O_3 as an additive, the oxidized layer was very thin, and was only several micrometers after 2000 h treatment. On the other hand, in the case of samples that had Y_2O_3 and Al_2O_3 as additives, the oxidized layer was very thick and had grown to about 30 μm after 2000 h. The thickness of the oxidized layers of specimens with SiC added were about 20–40% smaller than the specimens without SiC added.
(4) Oxidation kinetics of S-1 and S-2 obeyed a parabolic law on the whole, while those of S-3 and S-4 had a break between 500 and 1000 h.
(5) Examination of the cross sections of specimens showed that the "diffused layer", the concentration of Y and Al, decreased inside the base material, when specimen had both Y_2O_3 and Al_2O_3 as sintering additives. Moreover, the thickness of the SiC composite specimens was about 20–40% smaller than that of the non-composition.
(6) The thicknesses of the oxidized layer and the diffused layer were almost in proportionality, represented by "thickness of diffused layer" $= 0.85 \times$ "thickness of oxidized layer".
(7) The rate of the oxidation reaction on S-1and S-2 was mainly controlled by diffusion inside the oxidized layer. However, that on S-3 and S-4 was controlled by diffusion inside both oxidized layer and grain boundary of base material.

References

1. Ukyo, Y., The effect of a small amount of impurity on the oxidation of Si_3N_4 ceramics. *J. Mater. Sci.* 1997, **32**, 5483–5489.
2. Babini, G. N. and Vincenzini, P., In *Oxidation Kinetics of Hot-Pressed Silicon Nitride, Progress in Nittrogen Ceramics*, ed. F. L. Riley. Martinus Nijhoff Publishers, Boston, 1983, pp. 427–438.
3. Babini, G. N., Bellosi, A. and Vincenzini, P., A diffusion model for oxidation of hot-pressed Si_3N_4–Y_2O_3–SiO_2 materials. *J. Mater. Sci.* 1984, **19**, 1029–1042.
4. Cinibulk, M. K., Thomas, G. and Johnson, M. S., Oxidation behaviour of rare-earth disilicate Si_3N_4 ceramics. *J. Am. Ceram. Soc.* 1992, **75**(8), 2044–2049.
5. Mieskowski, D. M. and Sanders, W. A., Oxidation of silicon nitride sintered with rare-earth oxide additions. *J. Ame. Ceram. Soc. Commun.* 1985, **68**, 160–163.
6. Maeda, M., Nakamura, K. and Yamada, M., Oxidation resistance of silicon nitride ceramics with various additives. *J. Mater. Sci.* 1990, **25**, 3790–3794.
7. JIS B0601, *Geometrical Product Specifications (GPS)—Surface Texture: Profile Method—Terms, Definitions and Surface Texture Parameters*. Japanese Industrial Standard, 1996.
8. Hasegawa, Y., Oxidation behaviour of hot-pressed Si_3N_4 with addition of Y_2O_3 and Al_2O_3. *Yogyo* 1980, **88**(5), 292–297.
9. Costa Oliveira, F. A., Baxter, D. J. and Ungeheuer, J., Modelling of the oxidation kinetics of a Yttria-doped hot-pressed silicon nitride. *J. Eur. Ceram. Soc.* 1998, **18**, 2307–2312.
10. Tripp, W. C. and Graham, H. C., Oxidation of Si_3N_4 in the range 1300 to 1500 °C. *J. Am. Ceram. Soc.* 1976, **59**(9/10), 399–403.
11. Sata, T. and Fujii, K., Oxidations of silicon nitride, silicon oxynitride and sialon powders in atmospheres of O_2–N_2 system. *Yogyo* 1982, **90**(3), 110–118 (in Japanese).